Automated multimodal imaging of *Caenorhabditis elegans* behavior in multi-well plates

Hongfei Ji[a,b], Dian Chen[a], and Christopher Fang-Yen[a,b]

[a]Department of Biomedical Engineering, College of Engineering, The Ohio State University, Columbus, OH 43210, USA

[b]Department of Bioengineering, School of Engineering and Applied Science, University of Pennsylvania, Philadelphia, PA 19104, USA

ABSTRACT

Large-scale assays of behavior in model organisms play an important role in genetic screens, drug testing, and the elucidation of gene-behavior relationships. We have developed an automated, high-throughput imaging and analysis method for assaying behaviors of the nematode *C. elegans*. We use high-resolution optical imaging to longitudinally record the behaviors of 96 animals at a time in multi-well plates, and computer vision software to quantify the animals' locomotor activity, behavioral states, and egg laying events. To demonstrate the capabilities of our system we used it to examine the role of serotonin in *C. elegans* behavior. We found that egg-laying events are preceded by a period of reduced locomotion, and that this decline in movement requires serotonin signaling. In addition, we identified novel roles of serotonin receptors SER-1 and SER-7 in regulating the effects of serotonin on egg laying across roaming, dwelling, and quiescent locomotor states. Our system will be useful for performing genetic or chemical screens for modulators of behavior.

INTRODUCTION

C. elegans behavioral assays are widely used to study biological mechanisms in diverse areas such as aging (1, 2), sleep (3), development (4), and neurological disorders (5, 6). Assays of worm behavior have traditionally been done by manual assays and visual

observations, which are labor intensive, subject to observer error, and low in throughput due to examination of a single animal at a time.

To address these limitations, researchers have developed systems for analyzing worm behaviors via video recording and software analysis (7, 8). These include methods for imaging worms on standard agar plates (9–15), in microfluidic devices (16–21), and in multi-well substrates (1, 22–26).

Our laboratory has been conducting behavioral screens for the effect of genetic mutations and/or pharmacological compounds on various aspects of *C. elegans* behavior, including locomotion, egg laying, and behavioral states such as quiescence, dwelling, and roaming (1, 15, 21, 23, 27, 28). Toward this end, we sought to develop an efficient method for screening a large number of conditions for multiple behaviors simultaneously.

Here, we report a method for multimodal behavioral recording and analysis of *C. elegans* using 96-well plates. We developed a computer vision software toolbox to automate analysis of several behavioral metrics including locomotion activity, behavioral states, locomotor frequency, and egg laying. This automated approach is capable of continuously recording behaviors from 96 individual animals simultaneously for several hours under controlled conditions. We demonstrate the capabilities of this system by analyzing the roles of serotonin signaling in locomotor and egg-laying behaviors. Our findings underscore the extensive capabilities of longitudinal imaging systems for large-scale phenotypic assays.

RESULTS

System design for high-content imaging of multi-well assay platform

Our imaging platform contains a 20-megapixel CMOS camera, a C-mount lens, a 30 cm diameter LED ring illuminator, and a plate holder (Fig. 1A). One or more worms in liquid NGM media are prepared in each well of a 96-well plate and the plate is imaged under dark field illumination (Figs. 1 A and B). The platform components are positioned to visualize worms and embryos in each well while minimizing stray light from well edges (Fig. 1B).

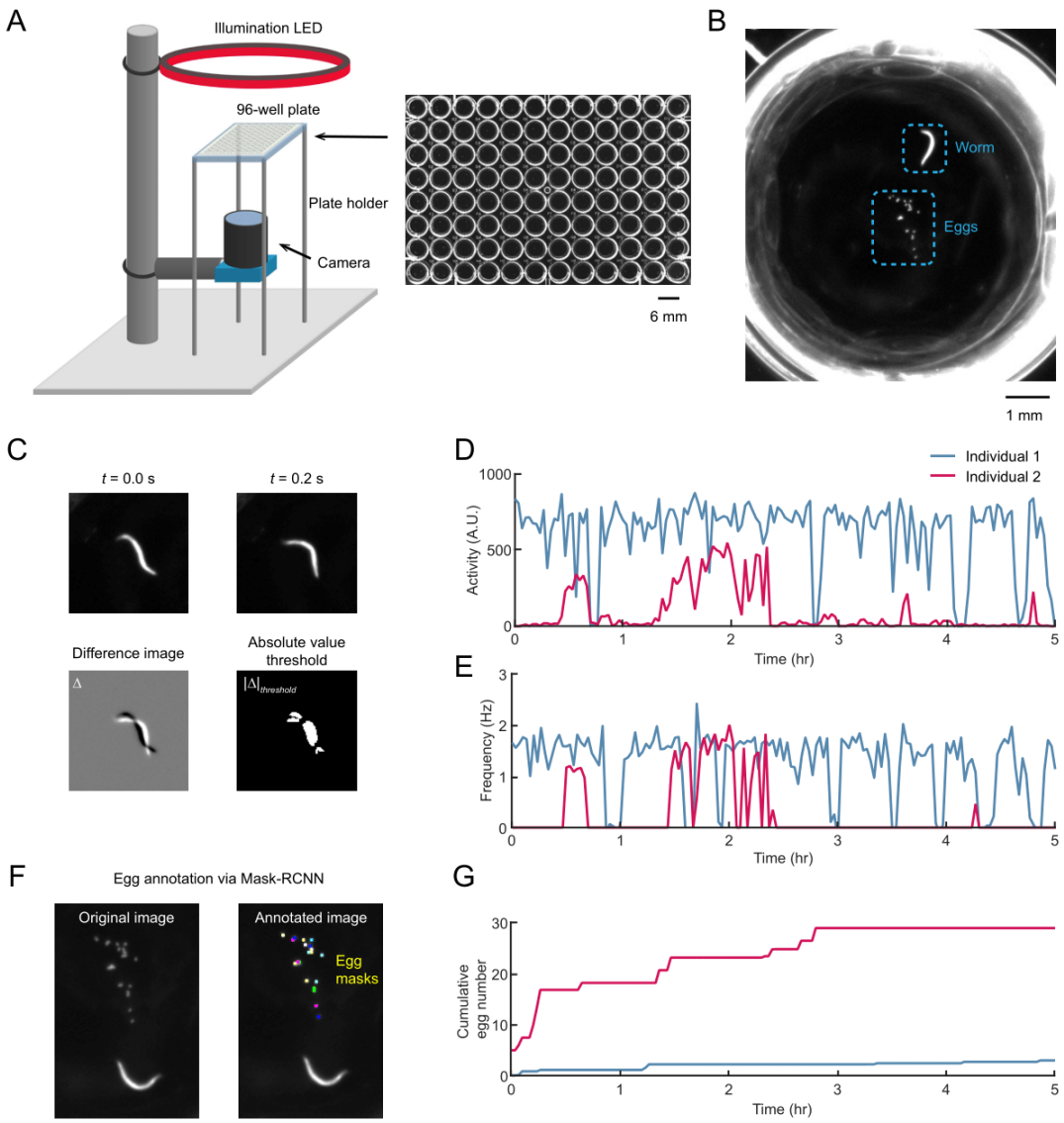

Figure 1. System design and behavioral quantification. (A) Schematic of the imaging system and image of a 96-well assay plate containing one worm per well. (B) Detail of a well containing a single 1-day adult and multiple eggs. (C) Activity is calculated as the sum of the number of pixels whose pixel value intensities change above a threshold. The change in the pixel value intensity is calculated by the pixel-by-pixel difference of temporally adjacent images. (D) Activity over time of two individual wild-type animals. (E) Locomotor frequency over time of two wild-type animals. (F) Egg detection via Mask R-CNN from the original video frame (*Left*). The egg objects are annotated with masks inferred by the model (*Right*). (G) Number of eggs laid for two wild-type animals.

Computer vision automates multimodal behavioral measurements

We developed image analysis software for quantifying animal locomotory and egg-laying behaviors within each well. Using a combination of computer vision algorithms and convolutional neural network (CNN), the software analyzes images to measure behavioral

parameters, including locomotion activity, locomotor frequency, and egg-laying rate (see *Methods*).

Locomotion activity is computed through pixel-by-pixel subtraction of consecutive video frames, with the activity defined by the number of pixels exhibiting intensity changes between subsequent frames (Figs. 1 C and D) (3). To measure locomotor frequency we used an algorithm based on analysis of image invariants (Fig. 1E) (29). The image analysis software also employs a Mask-Region Convolutional Neural Network (Mask-RCNN) to automatically annotate and enumerate worm embryos in each well (Figs. 1 F and G) (30, 31).

Evaluation of automated measurements

We tested the accuracy of our software in analyzing the locomotor frequency and egg-laying events by comparing the software's measurements with those obtained through human observation.

We evaluated the accuracy of automated frequency analysis by comparing it to manual counts of head bends in 480 video clips (each 6 s long) of individual wild-type worms across all 96 wells. The automated frequency results demonstrated good agreement with manual data with an overall root mean squared error of 0.097 Hz and an R-squared value of 0.964 (29). We found that locomotion activity is also highly correlated with locomotor frequency by comparing it with the ground-truth data (Fig. 2A).

To assess the accuracy of the egg-detector RCNN model, we applied it to identify and count eggs across all 96 wells of the plate. The collected well images contained 1-day-old adult wild-type worms alongside the eggs they laid, captured at 2 and 5 hours after animals were transferred into the assay plate. We found that the egg counts inferred by the model were in good agreement with those counted manually (Fig. 2B).

Together, the automated methods of our system accurately measure locomotion activity, locomotor frequency, and embryo numbers through longitudinal imaging.

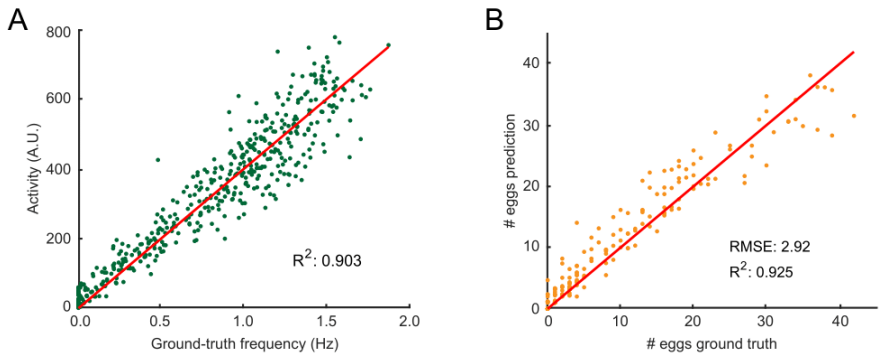

Figure 2. Evaluation of automated behavioral measurements. (A) Locomotion activity compared with the frequencies calculated by manual observation of recorded videos. (B) Egg numbers inferred by the Mask-RCNN model compared with those counted manually.

Automated tracking of locomotion, behavioral states, and egg laying

C. elegans locomotory and egg-laying behaviors are modulated by serotonergic, dopaminergic, and peptidergic signaling (32–34). The *C. elegans* nervous system uses serotonin (5-HT) to modulate both its locomotory and egg-laying behaviors, and external serotonin has been found to inhibit locomotion and stimulate egg-laying activity (23, 35–37).

To evaluate our system's reliability and capability for large-scale assays, we tracked the locomotion and egg-laying behaviors of wild-type and mutant *C. elegans* individuals under controlled serotonin conditions (see *Methods* and Figs. 3 A-F). Animals were individually housed in wells of an assay plate filled with liquid NGM and defined serotonin concentrations (5-HT-: 0 mM; 5-HT+: 6.5 mM). In each experiment, we monitored up to 96 animals for 5 h, which yielded 151 video clips with 5 fps and 20 s duration.

Both wild-type and mutant animals under serotonin-free conditions showed relatively active locomotion (Figs. 3 A and B) and low egg-laying rates (Fig. 3C). In contrast, the administration of exogenous serotonin induced diverse behavioral dynamics across the tested strains (Figs. 3 D-F).

We defined parameters for quantifying each animal's locomotory states (38). We calculated the mean of each animal's top 5% activity values across the experiment, and

112 used this value to define a normalized activity. This data allowed us to identify sedentary and
113 active bouts of locomotion using an empirical threshold (Fig. 3G) (23). We focused on
114 assessing the average locomotion activity, the fraction of time spent in the active state, and
115 the average locomotor frequency during the active state.

116 Wild-type and mutant animal populations exhibited diverse locomotion activity levels and
117 active locomotory states across genotypes and different levels of exogenous serotonin (Figs.
118 3 I and J). Both wild-type and mutant animals generally exhibited high activity levels and
119 spent the majority of time (over 78%) in the active state under the serotonin-free condition
120 (Figs. 3 I and J). With the addition of exogenous serotonin, activity levels and active state
121 fractions decreased in wild-type animals and in *egl-1* mutants (which lack HSN serotonergic
122 neurons that innervate egg-laying muscles) (Figs. 3 I and J). In contrast, *ser-1* and *ser-7*
123 mutants (deficient in G protein-coupled metabotropic receptors SER-1 and SER-7) exhibited
124 resistance to the effects of serotonin on locomotion activity and active state fractions, while
125 *ser-1;ser-7* double mutants showed enhanced resistance to exogenous serotonin (Figs. 3 I
126 and J). This result suggests that the SER-1 and SER-7 receptors play a role in mediating
127 inhibitory effects of external serotonin on locomotor behavior.

128 We calculated the average locomotor frequency of each animal during its active state.
129 The average active locomotor frequency of wild-type and all tested mutant strains showed
130 little or no change in response to exogenous serotonin (Fig. 3K). Therefore, unlike the active
131 state fraction, the active locomotor frequency remained largely constant, independent of
132 exogenous serotonin. This experiment suggests that external serotonin on locomotion
133 primarily affects initiation of activity rather than alteration of an established locomotor
134 rhythm.

135 To characterize the egg-laying dynamics of each animal, we calculated the average egg-
136 laying rate and the midpoint egg-laying time t_{50}, the time taken to reach half of the total
137 number of eggs laid during the experiment (Fig. 3H). Under serotonin-free conditions, wild-

type animals averaged an egg-laying rate of 1.2 eggs/h (Fig. 3L). The population's t_{50} values exhibited a biphasic distribution, with the majority displaying early midpoint egg-laying times (Fig. 3M). Compared to the wild type, the mutant animals tested had similar egg-laying rates but displayed different distributions in t_{50} (Figs. 3 L and M).

In the presence of exogenous serotonin, wild-type and *egl-1* mutant animals showed significant increases in egg-laying rates and decreases in t_{50} values (Figs. 3 L and M). The *ser-1* and *ser-7* mutants had a moderate increase in egg-laying rates in response to exogenous serotonin, while *ser-1;ser-7* double mutants maintained low egg-laying rates (Figs. 3L). The high degree of variation in the t_{50} distribution observed in the *ser-1*, *ser-7*, and *ser-1;ser-7* double mutants remained largely consistent with the addition of exogenous serotonin (Figs. 3M). This result indicates that SER-1 and SER-7 receptors may be necessary for normal serotonin-mediated egg laying involving both egg-laying rates and temporal patterns.

In summary, our behavioral findings qualitatively agree with previously reported results for each strain, encompassing behavioral parameters like locomotory state, locomotor frequency, and egg-laying rate, as well as the effects of exogenous serotonin (4, 22, 27, 35, 37, 39–41). These experiments demonstrate our system's reliability, scalability, and efficiency in concurrently and longitudinally assessing multi-metric behavioral dynamics.

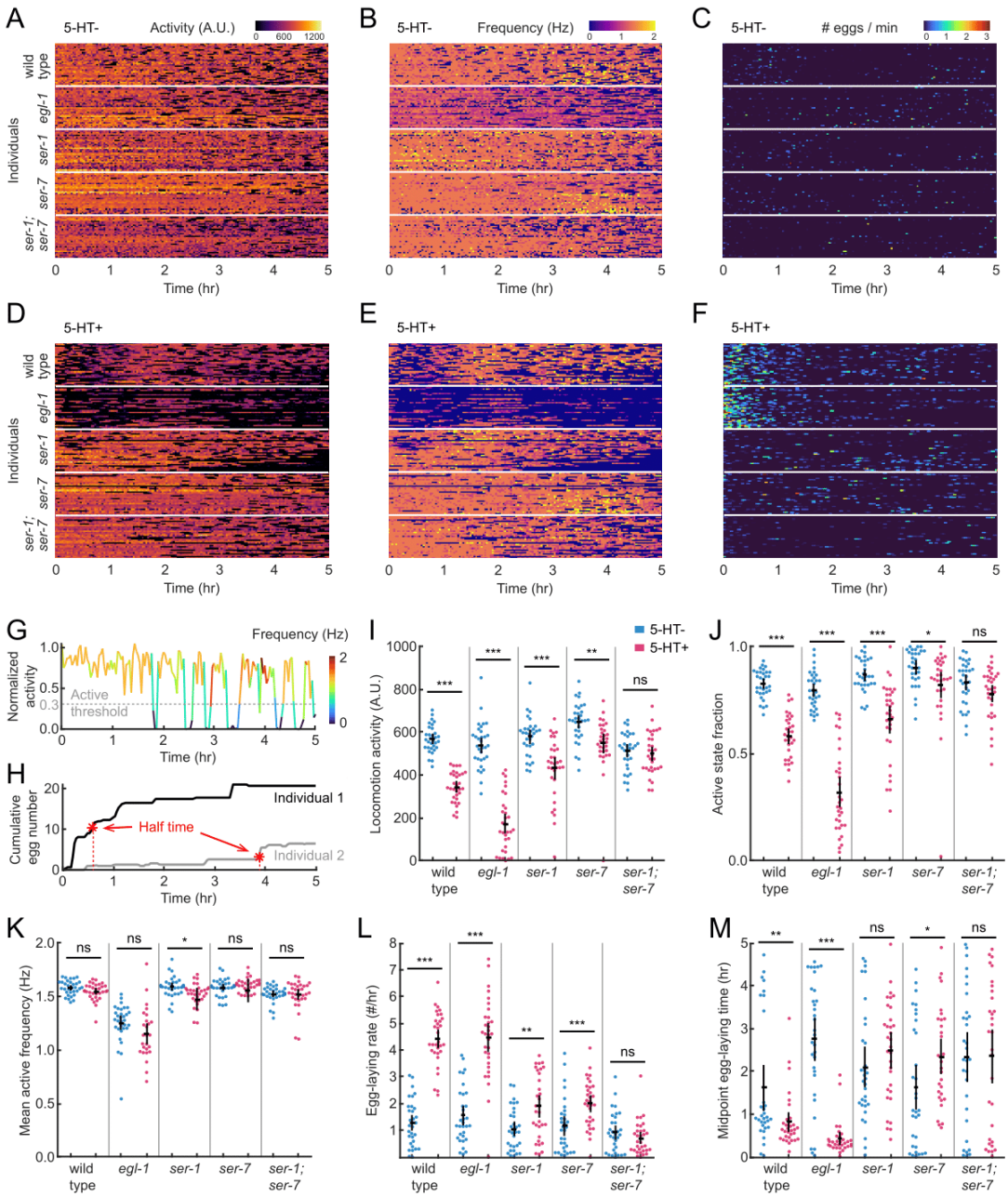

Figure 3. Automated large-scale tracking of locomotory and egg-laying behaviors. (A-C) Heat maps of activity (A), locomotor frequency (B), and egg-laying rate (C) for wild-type and mutant individuals (n = 32 for each strain group). Each row in the heatmap shows the behavioral dynamics of a single animal. (D-F) Same as (A-C), but for animals in an exogenous serotonin environment. (G) Normalized activity over time for an individual. The data is normalized by the mean value of the 95th to 100th percentile of all activity values observed during the experiment. Color represents the locomotor frequency of the individual. Gray dashed line indicates the threshold value of normalized activity above which locomotion bouts are labeled as active states. (H) Cumulative number of eggs released by two individuals. Red asterisk indicates midpoint egg-laying time (t_{50}), the time taken to reach one-half of the total egg number accumulated at t = 5 h. (I) Locomotion activity of wild-type and mutant

individuals. (J) Fraction of time during active state of wild-type and mutant individuals. (K) Mean locomotor frequency during active state of wild-type and mutant individuals. (L) Egg-laying rate of wild-type and mutant animals. (M) Midpoint egg-laying time (t_{50}) of wild-type and mutant individuals. In (I-M), each point represents an animal, red and blue indicate groups in the respective serotonin conditions, black bars represent population mean ± SEM. *p < 0.05, **p < 0.01, ***p < 0.001.

Serotonin is required for preparatory movement decline during egg-laying

One advantage of our system is that it is capable of capturing locomotor and egg-laying behaviors simultaneously. We examined the temporal correlation between locomotion and egg-laying by extracting the locomotion pattern before and after each egg-laying event throughout the recording period (Figs. 4 A and B). The average locomotor activity of wild-type animals was found to decrease approximately 10 min prior to egg-laying events, with the minimum activity reached roughly at the time the egg(s) were laid and subsequently recovering to a baseline value within about 10 min (Fig. 4C). Observation of the video clips revealed that the activity of individual animals during egg-laying events was consistently lower than during adjacent periods during which no eggs were laid (individual traces in Fig. 4C). Notably, nearly every egg-laying event was preceded by a decline in activity, although the magnitude and timing of the maximal activity drop varied substantially both within individual animals and among different animals (Fig. 4C).

Since serotonin functions in circuits that control *C. elegans* locomotion and egg laying (4, 35, 37, 38, 42), we examined the effects of serotonin and the neurons regulating egg-laying behavior on the control of locomotion. We asked how exogenous serotonin might modulate the observed correlation between locomotion and egg-laying. In the presence of exogenous serotonin the decline in movement around egg-laying events was more pronounced. Furthermore, the timing of the activity decline and subsequent recovery occurred approximately 4 min earlier than without exogenous serotonin (Fig. 4D).

Next, we explored the effects of endogenous serotonin signaling on the coordination between egg-laying and locomotion. We analyzed mutant animals deficient in serotonin due

193 to a mutation in the biosynthetic enzyme tryptophan hydroxylase (TPH-1). While the overall
194 locomotion of *tph-1* mutants appeared normal (14), these mutants did not exhibit a decline in
195 movement around egg-laying events (Fig. 4E). The introduction of exogenous serotonin
196 restored this coordination deficit (Fig. 4F). Together, these results show that serotonin
197 signaling is required for the observed decline in movement during egg-laying events.

198 We further investigated the effects of neurons that regulate egg-laying behavior on the
199 coordination with locomotion, focusing on the role of HSNs, a pair of serotonergic neurons
200 crucial for a normal egg-laying process. We observed the behavior of *egl-1* mutants, which
201 specifically lack HSNs. While *egl-1* mutants did exhibit a decline in movement around egg-
202 laying events, the timing of their minimum activity was delayed, occurring consistently after
203 egg-laying (Fig. 4G). Administering exogenous serotonin to these groups restored the timing
204 delay (Fig. 4H). These results suggest that HSNs may play a modulatory role in coordinating
205 the interaction between egg laying and locomotion.

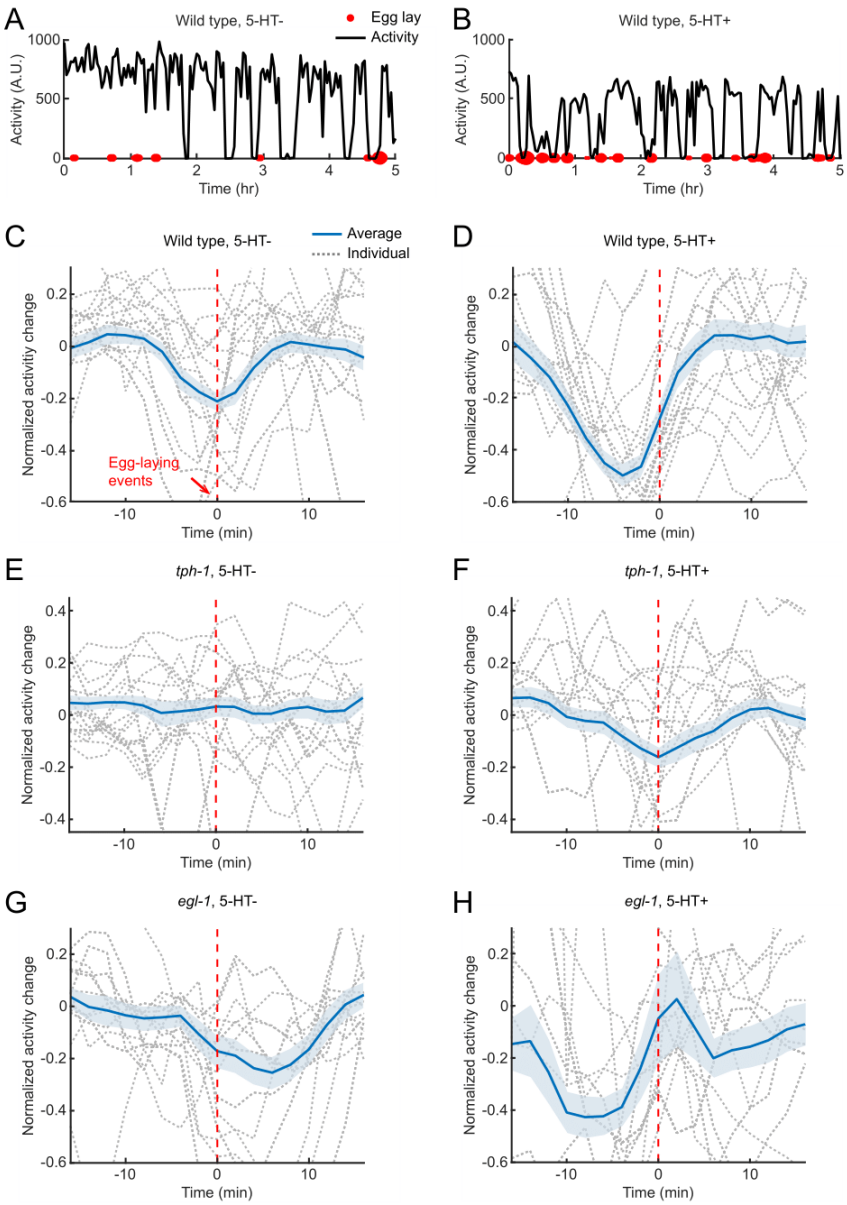

Figure 4. Serotonin is required for preparatory movement decline during egg laying. (A and B) Locomotion activity and egg-laying dynamics for two individual wild-type animals in either the absence (A) or presence (B) of exogenous serotonin (B). Black curves represent activity trajectories. Red dots indicate egg-laying events scored by automated method, and dot size is used to visualize the egg-laying rate. (C and D) Average normalized activity change around egg-laying events (red dashed line, aligned at $t = 0$) of wild-type animals (n = 32) in either the absence (C) or presence (D) of exogenous serotonin. Blue line and shaded area indicate population mean ± SEM. Gray dashed curves represent 20 randomly selected individual trajectories for each group. (E and F) Same as (C and D), but for *tph-1* mutant animals (n = 32). (G and H) Same as (C and D), but for *egl-1* mutant animals (n = 32).

The metabotropic serotonin receptors SER-1 and SER-7 regulate serotonin effects on reproduction in separate locomotory states

Our analyses of *C. elegans* locomotion activity and behavioral states showed that animals occasionally alternated between sedentary and active states (Figs. 3 A, D, and G). This alternation between states was influenced by exogenous serotonin and seemed to happen at a frequency similar to that of egg-laying events (Figs. 4 A and B). We asked whether there is a correlation between *C. elegans* egg-laying behavior and behavioral states and whether one is influenced or modulated by the other.

We discerned sedentary and active periods from the locomotion activity trajectories of individual animals and registered these periods with their respective egg-laying rates (Figs. 5 A and B). We noted that in serotonin-free environments, wild-type animals spent the majority of their time in the active state (Fig. 5A) and laid more eggs during these active periods (Fig. 5C). Conversely, in environments with exogenous serotonin, animals spent nearly equal amounts of time on sedentary and active states (Fig. 5B), with more eggs being laid during the sedentary states (Fig. 5C).

To compare the egg-laying activity between different locomotory states, we calculated the egg laying rate by dividing the total egg count during each state with the corresponding state duration. The data revealed that, irrespective of exogenous serotonin, wild-type animals consistently exhibited higher egg-laying rates during sedentary locomotor state (Fig. 5D).

The observed dual role of serotonin in regulating both locomotory states and egg-laying behavior (as shown in Figs. 5 A and B) prompted a closer examination of serotonin signaling in modulating the observed dependence of egg-laying behavior on locomotory states (Figs. 4C and 5D). We revisited the behavioral recordings of HSN-defective mutants (*egl-1*) and serotonin receptor mutants (*ser-1*, *ser-7*, and *ser-1;ser-7*), with a particular focus on the effects of exogenous serotonin on the egg-laying rate during distinct locomotory states. By

242 registering the egg-laying rate over time for each mutant individual and correlating it with the
243 respective locomotory states, we observed that both wild-type and *egl-1* mutant animals
244 experienced a significant increase in egg-laying rate during both sedentary and active states
245 when exposed to exogenous serotonin (Figs. 5 E and F). Interestingly, the *ser-1* and *ser-7*
246 mutants resisted the effects of exogenous serotonin on their egg-laying rates, but each
247 during one of the two states (Figs. 5 E and F). Meanwhile, the *ser-1;ser-7* double mutants
248 resisted the egg-laying effects of exogenous serotonin during both states (Figs. 5 E and F).

249 In summary, our findings suggest that *C. elegans* preferentially lay eggs during the
250 sedentary state, with serotonin receptors SER-1 and SER-7 distributing the effects of
251 serotonin on egg-laying behavior across distinct locomotory states.

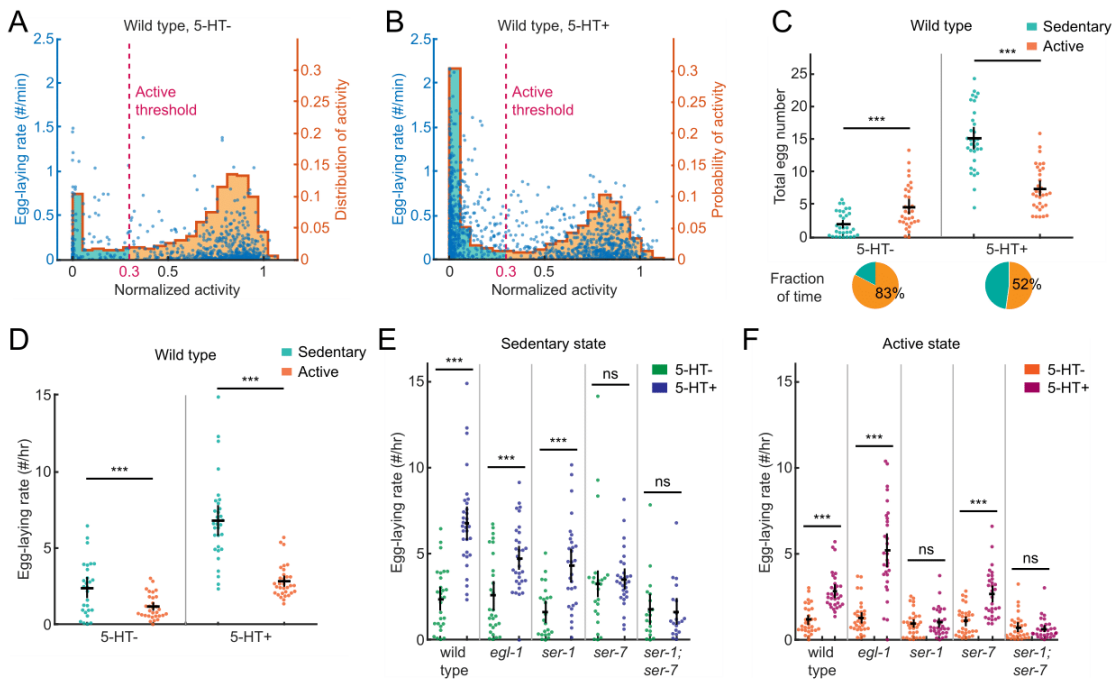

252

253 **Figure 5. Receptors SER-1 and SER-7 regulate serotonin effects on reproduction in separate locomotory**
254 **states.** (A and B) Histogram of normalized activity (orange stairstep curve, right-side y-axis) and scatter plot
255 showing egg-laying rate versus normalized activity value (blue dot, left-side y-axis) for wild-type animals in either
256 the absence (A) or presence (B) of exogenous serotonin. In histograms, the height of the stairstep denotes the
257 relative probability of each of 20 bins of normalized activity, red dashed line indicates the threshold value of
258 normalized activity above which locomotion is flagged as active state, green and orange shaded areas represent
259 proportions of sedentary and active states. In scatter plots, each point represents a 20-sec bout of an individual

animal (n = 4832 bouts from 32 animals for each condition). (C) (*Upper*) Total number of eggs released by wild-type animals during sedentary or active states in either the absence or presence of exogenous serotonin. (*Lower*) Fraction of time of sedentary versus active states in respective serotonin conditions. (D) Egg-laying rate of wild-type animals during sedentary or active states in either the absence or presence of exogenous serotonin. (E and F) Egg-laying rate of wild-type and mutant individuals during sedentary (E) or active (F) state in either the absence or presence of exogenous serotonin. In (C-F), each point represents an animal, black bars represent population mean ± SEM. ***$p < 0.001$.

DISCUSSION

Our automated image recording and analysis system, set within the conventional 96-well plates, yielded substantial benefits in throughput, preservation of animal individuality, multi-metric behavioral output, and manageable and controlled external conditions. Our system facilitates the individual evaluation of parameters involving locomotion activity, behavioral states, and egg-laying behavior. This allows for the identification of diverse locomotion and reproduction characteristics across individuals and populations.

We obtained large-scale longitudinal behavioral recordings of individual animals through high-resolution imaging. The integrated computer-vision software toolkit automates quantifying various behaviors, leveraging accurate assessments of animal motility, locomotor rhythmicity, and egg laying. Applications enabled by our method included pharmacological screens (43), screening genes essential for diverse neural functions (44), and studies of complex behavioral patterns and states (45).

From our experimental demonstrations, we observed that wild type animals exhibit a decline in movement decline during the egg-laying process. This finding diverges from those of previous analyses in which locomotion was observed to increase around egg-laying events (23, 40). This discrepancy may stem from variations in experimental food conditions; while our studies monitored animals in food-free environments, prior experiments involved animals on food, potentially altering their basal neural and behavioral states.

286 Our automated imaging and analysis pipeline is scalable, platform-independent, and built
287 from off-the-shelf parts. It is compatible with other standard or customized multi-array setups
288 used for large-scale behavioral assays (1). Additionally, its modular analysis algorithm and
289 customizable hardware configuration should allow for the integration of complex image-
290 analysis routines specific to various screening tasks. It also presents a versatile tool
291 adaptable to studying not just various sizes of *C. elegans* but potentially also other small
292 organisms like *Drosophila melanogaster* and its larvae.

293 Our multi-array and multi-metric behavioral tracking automation should facilitate rapid
294 execution of large, complex compound or genetic screens, making it possible to detect
295 subtle phenotypes that are usually difficult to identify with single-metric behavioral tracking
296 prevalent in existing systems. By assessing both locomotory and egg-laying activities, for
297 example, one can screen for mutants that have altered coordination between the two
298 behaviors or that exhibit subtle behavioral changes that target multiple respective
299 neurochemical signaling systems.

300 **METHODS**

301 ***C. elegans* strains and maintenance**

302 *C. elegans* strains were cultivated on *Escherichia coli* strain OP50 at 20 °C using standard
303 conditions (46). The wild-type strain (Bristol N2) and mutant strains used in this work were
304 obtained from the NIH *Caenorhabditis* Genetics Center. Mutant trains used in behavioral
305 assays are the following: MT1082 *egl-1(n487)*, DA1814 *ser-1(ok345)*, DA2100 *ser-*
306 *7(tm1325)*, DA2109 *ser-7(tm1325); ser-1(ok345)*. All experiments were performed with 1-
307 day-old adult animals. Worm populations were synchronized by timed egg lays according to
308 standard methods (47).

309 **Multi-well plate assays**

310 To study the effect of various chemicals on egg-laying and locomotion behaviors, we used
311 96-well microtiter assay plates (Corning 3795, round bottom), with each well containing an

312 indicated number of worms immersed in 60 μL of NGM buffer dissolved with the chemical of
313 interest. The liquid NGM buffer consists of the same ingredients as solid NGM but without
314 agar, peptone, or cholesterol (48).

315 **Image data acquisition and processing**

316 The assay plate was placed on a platform within a custom-built imaging system. Dark-field
317 illumination was generated by an LED light ring (outer diameter 12 inches; Sunpak) above
318 the platform. A video was captured using a CMOS camera (DMK 33UX183, The Imaging
319 Source) with a C-mount lens (Fujinon HF12.5SA-1, focal length 35 mm, f/2.8 or Nikon, focal
320 length 55 mm, f/3.5 F-mount lens with a C-mount adapter) for 20 sec at 5 framerate
321 operated with IC Capture imaging software (The Imaging Source). A whole course of
322 behavioral assay was performed by capturing a sequence of the 20 s videos, each of which
323 was taken every 2 min for 5 h of recording time. The field of view of the system was set to
324 display all 96 wells of the plate, which yields an 18 μm pixel resolution.

325 Video imaging data from the assay plate was analyzed using custom-written MATLAB
326 and Python software. The behavioral outcomes from the analysis include locomotion activity,
327 locomotor frequency, and egg-laying behavior. Locomotion activity is defined as the number
328 of pixels whose intensity changes between subsequent image frames due to worms'
329 movements (1, 3). Locomotor frequency is calculated by our automated image analysis
330 software capable of rapidly estimating rhythmic behaviors (29). Egg-laying behavior is
331 quantified by the number of eggs released into the environment. Eggs are detected by a
332 trained mask-regional convolutional neural network (Mask-RCNN) (31).

333 **Measuring locomotory behavior**

334 We calculated locomotor activity using previously described methods (3, 27). Pairs of
335 temporally adjacent video images were subtracted to generate difference images, which
336 were then divided by the average pixel intensity, yielding normalized maps of pixel value
337 intensity change. A Gaussian smoothing filter with a standard deviation of one pixel was

338 applied to decrease image noise. A binary threshold was applied to the filtered image to
339 determine the presence or absence of movement at each pixel location. The sum of all
340 pixels exhibiting movement was calculated as the locomotor activity.

341 To calculate locomotor frequency we used our custom algorithm Imaginera (image
342 invariants ensemble for rhythmicity analysis) (29). For each video frame, our algorithm
343 estimates the pixel area of a worm (A_{worm}) in each well. When animals approached the
344 edge of wells, they were occasionally occluded such that the animals could not be easily
345 observed, decreasing A_{worm}. To mitigate the influence of this occlusion, we censored any
346 frames during which A_{worm} was smaller than a preset empirical threshold when calculating
347 locomotor activity or frequency.

348 **Measuring egg-laying behavior**

349 To evaluate egg-laying behavior, we counted the eggs that have been released into each
350 well in 20 s videos. Each video was sampled by 5 images that are linearly spaced across the
351 20 s period, with adjacent images separated by 4 sec. Following previously described
352 methods (30), we deployed a mask-regional convolutional neural network (Mask-RCNN) to
353 detect and identify eggs in each image. The Mask-RCNN model was trained, evaluated, and
354 deployed by PyTorch GPU (v2.0.0 + cu1.1.8) on a system equipped with a 13th Intel(R)
355 Core(TM) i7-13700K processor and an NVIDIA GeForce RTX 4080 GPU.

356 For the model training, 1653 cropped single-well images (containing eggs and worms)
357 from 18 videos in all 96 distinct well positions were manually annotated and saved as
358 training datasets using a Python annotation package. We augmented the training set using
359 operations including flipping, intensity adjustment, and Gaussian blurring, yielding a total of
360 6612 annotated images in the dataset. The model was trained for 25 epochs, during which
361 the training set was randomly divided into training and testing sets with an 80/20 split ratio
362 (5290 images for training, 1322 images for testing). We evaluated the Mask-RCNN model
363 using characterization metrics, including precision, recall, and average precision (AP) (49).

With the trained Mask-RCNN model, the egg number in an image was determined by $N_{RCNN} = A_{RCNN}/a_0$, where A_{CNN} represents the pixel number of egg objects inferred by the model, and a_0 is the pixel number of a single egg, estimated by $a_0 = \sum A_{train}N_{train} / \sum N_{train}^2$. Here, $\sum A_{train}N_{train}$ is the sum of the products of egg pixel number and egg number manually counted from individual images in the training set, and $\sum N_{manual}$ is the sum of egg numbers from the same set.

Mask R-CNN model characterization

We evaluated how well our model performed by calculating precision and recall as well as average precision (AP). Precision is the proportion of true positive predictions (correctly detected objects) among all positive predictions (correctly detected objects plus false positives). Recall is the proportion of true positive predictions among all actual positive instances (true positives plus false negatives). Average precision is calculated by computing the area under the Precision-Recall curve through the following steps: (a) For each confidence threshold, calculate precision and recall. (b) Interpolate the precision values by taking the maximum precision for any recall value greater than the current recall value. (c) Compute the area under the interpolated Precision-Recall curve using numerical integration.

To determine true positives (TP), false positives (FP), and false negatives (FN), we used the Intersection-over-Union (IoU) threshold, which measures the overlap of the ground truth bounding box and the prediction bounding box (49). An egg detection is considered a TP if its IoU with the corresponding ground-truth bounding box is greater than or equal to the IoU threshold. If the IoU is below the threshold, it is considered an FP. An FN is a ground-truth bounding box that does not have a corresponding detection. An IoU threshold of 0.3 and a confidence score threshold of 0.01 were used for our egg-detection model.

Experimental design and statistical analyses

Behavioral comparisons in locomotion activity, active state fraction, locomotor frequency, and egg-laying rate (Figs. 3 I-L, Figs. 5 C-F) were performed using a two-tailed Student's *t*-

test. Differences in midpoint egg-laying time distributions (Fig. 3M) were compared using a Wilcoxon rank sum test.

DATA AVAILABILITY

Strains are available upon request. The software and experimental sample data are available at https://github.com/cfangyen/multiwell.

ACKNOWLEDGMENTS. We thank Niels Ringstad, Yen-Chih Chen, Mohammad Seyedsayamdost, Andrew Ruba, and Miriam Goodman for providing reagents and helpful advice. Some strains were provided by the *C. elegans* Genetic Center, funded by the NIH Office of Research Infrastructure Programs (P40 OD010440). This work was funded by the National Institutes of Health (R01DA056358).

REFERENCES

1. M. A. Churgin, *et al.*, Longitudinal imaging of Caenorhabditis elegans in a microfabricated device reveals variation in behavioral decline during aging. *Elife* **6**, e26652 (2017).

2. N. Stroustrup, *et al.*, The Caenorhabditis elegans lifespan machine. *Nature methods* **10**, 665–670 (2013).

3. D. M. Raizen, *et al.*, Lethargus is a Caenorhabditis elegans sleep-like state. *Nature* **451**, 569–572 (2008).

4. S. Stern, C. Kirst, C. I. Bargmann, Neuromodulatory control of long-term behavioral patterns and individuality across development. *Cell* **171**, 1649–1662 (2017).

5. S. Mondal, *et al.*, Large-scale microfluidics providing high-resolution and high-throughput screening of Caenorhabditis elegans poly-glutamine aggregation model. *Nature communications* **7**, 13023 (2016).

414 6. F. Calahorro, M. Ruiz-Rubio, Caenorhabditis elegans as an experimental tool for the
415 study of complex neurological diseases: Parkinson's disease, Alzheimer's disease and
416 autism spectrum disorder. *Invertebrate neuroscience* **11**, 73–83 (2011).

417 7. C. J. Cronin, Z. Feng, W. R. Schafer, "Automated Imaging of *C. elegans* Behavior" in *C.*
418 *Elegans*, (Humana Press, 2006), pp. 241–252.

419 8. S. J. Husson, W. S. Costa, C. Schmitt, A. Gottschalk, Keeping track of worm trackers.
420 *WormBook: The Online Review of C. elegans Biology [Internet]* (2018) (December 18,
421 2023).

422 9. N. Cermak, *et al.*, Whole-organism behavioral profiling reveals a role for dopamine in
423 state-dependent motor program coupling in C. elegans. *Elife* **9**, e57093 (2020).

424 10. C. J. Cronin, *et al.*, An automated system for measuring parameters of nematode
425 sinusoidal movement. *BMC genetics* **6**, 1–19 (2005).

426 11. L. Luo, *et al.*, Bidirectional thermotaxis in Caenorhabditis elegans is mediated by
427 distinct sensorimotor strategies driven by the AFD thermosensory neurons.
428 *Proceedings of the National Academy of Sciences* **111**, 2776–2781 (2014).

429 12. G. J. Stephens, B. Johnson-Kerner, W. Bialek, W. S. Ryu, Dimensionality and
430 dynamics in the behavior of C. elegans. *PLoS computational biology* **4**, e1000028
431 (2008).

432 13. N. A. Swierczek, A. C. Giles, C. H. Rankin, R. A. Kerr, High-throughput behavioral
433 analysis in C. elegans. *Nature methods* **8**, 592–598 (2011).

434 14. E. Yemini, T. Jucikas, L. J. Grundy, A. E. Brown, W. R. Schafer, A database of
435 Caenorhabditis elegans behavioral phenotypes. *Nature methods* **10**, 877–879 (2013).

436 15. H. Ji, *et al.*, Phase response analyses support a relaxation oscillator model of
437 locomotor rhythm generation in Caenorhabditis elegans. *Elife* **10**, e69905 (2021).

438 16. D. R. Albrecht, C. I. Bargmann, High-content behavioral analysis of Caenorhabditis
439 elegans in precise spatiotemporal chemical environments. *Nature methods* **8**, 599–605
440 (2011).

441 17. S. H. Chalasani, *et al.*, Dissecting a circuit for olfactory behaviour in Caenorhabditis
442 elegans. *Nature* **450**, 63–70 (2007).

443 18. K. Chung, M. M. Crane, H. Lu, Automated on-chip rapid microscopy, phenotyping and
444 sorting of C. elegans. *Nature methods* **5**, 637–643 (2008).

445 19. M. Doitsidou, N. Flames, A. C. Lee, A. Boyanov, O. Hobert, Automated screening for
446 mutants affecting dopaminergic-neuron specification in C. elegans. *Nature methods* **5**,
447 869–872 (2008).

448 20. S. E. Hulme, S. S. Shevkoplyas, J. Apfeld, W. Fontana, G. M. Whitesides, A
449 microfabricated array of clamps for immobilizing and imaging C. elegans. *Lab on a*
450 *Chip* **7**, 1515–1523 (2007).

451 21. H. Ji, A. D. Fouad, Z. Li, A. Ruba, C. Fang-Yen, A proprioceptive feedback circuit
452 drives Caenorhabditis elegans locomotor adaptation through dopamine signaling.
453 *Proceedings of the National Academy of Sciences* **120**, e2219341120 (2023).

454 22. Y.-C. Chen, M. R. Seyedsayamdost, N. Ringstad, A microbial metabolite synergizes
455 with endogenous serotonin to trigger C. elegans reproductive behavior. *Proc Natl Acad*
456 *Sci U S A* **117**, 30589–30598 (2020).

457 23. R. J. McCloskey, A. D. Fouad, M. A. Churgin, C. Fang-Yen, Food responsiveness
458 regulates episodic behavioral states in Caenorhabditis elegans. *Journal of*
459 *Neurophysiology* **117**, 1911–1934 (2017).

24. A. D. Fouad, *et al.*, High-throughput imaging of Caenorhabditis elegans aging using collective activity monitoring. *bioRxiv*, 2021–10 (2021).

25. S. Harrington, *et al.*, Egg-laying and locomotory screens with C. elegans yield a nematode-selective small molecule stimulator of neurotransmitter release. *Communications Biology* **5**, 865 (2022).

26. E. Fryer, *et al.*, An efficient behavioral screening platform classifies natural products and other chemical cues according to their chemosensory valence in C. elegans. *bioRxiv* (2023) (November 9, 2023).

27. M. A. Churgin, R. J. McCloskey, E. Peters, C. Fang-Yen, Antagonistic serotonergic and octopaminergic neural circuits mediate food-dependent locomotory behavior in Caenorhabditis elegans. *Journal of Neuroscience* **37**, 7811–7823 (2017).

28. A. D. Fouad, *et al.*, Distributed rhythm generators underlie Caenorhabditis elegans forward locomotion. *Elife* **7**, e29913 (2018).

29. H. Ji, D. Chen, C. Fang-Yen, Segmentation-free measurement of locomotor frequency in Caenorhabditis elegans using image invariants. *bioRxiv*, 2024–01 (2024).

30. Z. Li, *et al.*, A robotic system for automated genetic manipulation and analysis of Caenorhabditis elegans. *PNAS nexus* **2**, pgad197 (2023).

31. K. He, G. Gkioxari, P. Dollár, R. Girshick, Mask r-cnn in *Proceedings of the IEEE International Conference on Computer Vision*, (2017), pp. 2961–2969.

32. S. Brenner, The genetics of Caenorhabditis elegans. *Genetics* **77**, 71–94 (1974).

33. D. J. McFarland, Decision making in animals. *Nature* **269**, 15–21 (1977).

34. M. Zhen, A. D. Samuel, C. elegans locomotion: small circuits, complex functions. *Current opinion in neurobiology* **33**, 117–126 (2015).

483 35. H. R. Horvitz, M. Chalfie, C. Trent, J. E. Sulston, P. D. Evans, Serotonin and
484 octopamine in the nematode Caenorhabditis elegans. *Science* **216**, 1012–1014 (1982).

485 36. W. R. Schafer, C. J. Kenyon, A calcium-channel homologue required for adaptation to
486 dopamine and serotonin in Caenorhabditis elegans. *Nature* **375**, 73–78 (1995).

487 37. C. Trent, N. Tsung, H. R. Horvitz, Egg-laying defective mutants of the nematode
488 Caenorhabditis elegans. *Genetics* **104**, 619–647 (1983).

489 38. S. W. Flavell, *et al.*, Serotonin and the neuropeptide PDF initiate and extend opposing
490 behavioral states in C. elegans. *Cell* **154**, 1023–1035 (2013).

491 39. L. Carnell, J. Illi, S. W. Hong, S. L. McIntire, The G-protein-coupled serotonin receptor
492 SER-1 regulates egg laying and male mating behaviors in Caenorhabditis elegans.
493 *Journal of Neuroscience* **25**, 10671–10681 (2005).

494 40. L. A. Hardaker, E. Singer, R. Kerr, G. Zhou, W. R. Schafer, Serotonin modulates
495 locomotory behavior and coordinates egg-laying and movement inCaenorhabditis
496 elegans. *J. Neurobiol.* **49**, 303–313 (2001).

497 41. R. J. Hobson, *et al.*, SER-7, a Caenorhabditis elegans 5-HT7-like receptor, is essential
498 for the 5-HT stimulation of pharyngeal pumping and egg laying. *Genetics* **172**, 159–169
499 (2006).

500 42. E. R. Sawin, R. Ranganathan, H. R. Horvitz, C. elegans locomotory rate is modulated
501 by the environment through a dopaminergic pathway and by experience through a
502 serotonergic pathway. *Neuron* **26**, 619–631 (2000).

503 43. T. Kaletta, M. O. Hengartner, Finding function in novel targets: C. elegans as a model
504 organism. *Nature reviews Drug discovery* **5**, 387–399 (2006).

44. C. I. Bargmann, E. Marder, From the connectome to brain function. *Nature methods* **10**, 483–490 (2013).

45. G. Haspel, *et al.*, To reverse engineer an entire nervous system (2023) (September 29, 2023).

46. J. Sulston, J. Hodgkin, The nematode Caenorhabditis elegans (1988).

47. S. Gandhi, J. Santelli, D. H. Mitchell, J. W. Stiles, D. R. Sanadi, A simple method for maintaining large, aging populations of Caenorhabditis elegans. *Mechanisms of ageing and development* **12**, 137–150 (1980).

48. T. Stiernagle, *Maintenance of C. elegans (February 11, 2006), WormBook, ed. The C. elegans Research Community, WormBook, doi/10.1895/wormbook. 1.101. 1* (2006).

49. K. Bates, K. N. Le, H. Lu, Deep learning for robust and flexible tracking in behavioral studies for C. elegans. *PLOS Computational Biology* **18**, e1009942 (2022).